Absolute dating of an Early Paleolithic site in Western Africa based on the radioactive decay of in situ-produced 10Be and 26Al

Anne-Elisabeth Lebatard, Didier Bourles, Regis Braucher

Nuclear Inst. and Methods in Physics Research B 456 (2019) 169–179

Contents lists available at ScienceDirect

Nuclear Inst. and Methods in Physics Research B

journal homepage: www.elsevier.com/locate/nimb

Absolute dating of an Early Paleolithic site in Western Africa based on the radioactive decay of in situ-produced ^{10}Be and ^{26}Al

Anne-Elisabeth Lebatard*, Didier L. Bourlès, Régis Braucher, Aster Team[1]

Aix Marseille Univ, CNRS, IRD, INRA, Coll France, CEREGE, Aix-en-Provence, France

ARTICLE INFO

Keywords:
Angola
Cosmogenic nuclides
Burial dating
Lower Paleolithic

ABSTRACT

Along the Angolan coast, the Early Paleolithic sites of Dungo IV and V (Baia Farta, Benguela) have delivered a rich pre-Acheulean lithic industry testifying the antiquity of the hominin settlement in western Africa despite the current absence of any hominin fossil in the area. In Dungo IV, the Paleolithic level is located on a conglomeratic paleo-beach (104 m a.s.l.) buried under an at least 3 m thick sandy layer. In Dungo V, two unearthed large whale fossils are associated with numerous lithic tools intimately mixed with the whale bones. This is the oldest evidence of stranded marine mammal scavenging by hominins in this part of Africa. The lack of volcanism and fossils makes chronological constrain difficult. Considering its configuration, the Dungo IV site may be relevant for a dating based on both the ^{10}Be and ^{26}Al cosmogenic nuclides. For this purpose, a depth profile all along the sandy layer overlying the archeological layer has been sampled. Statistical treatments performed on the ^{26}Al/^{10}Be ratios obtained for the depth profile demonstrate that they all belong to the same population. If we consider that the samples have always been at or close to their sampling depth, the regression modeling allows computing that the surface sedimentary layer has been emplaced at least 614 ka ago and less than 662 ka ago. On the other hand, if we consider that the surface deposit has been truncated, burial durations ranging from 585 ka to 786 ka and truncations lower than 4 m result from the modeling of the evolution of the ^{10}Be and ^{26}Al concentrations as a function of depth.

The analyses of four pre-Acheulean artefacts lead to a minimum burial duration of 730 ka and a maximum burial duration of 2.11 Ma.

The low pre-burial denudation rates modeled from the data acquired for the stone tools as well as for the overlying layer (1–16 m.Ma^{-1}) imply large inherited ^{26}Al and ^{10}Be concentrations. The post-depositional maximum denudation rate of 71 m.Ma^{-1} associated with both the lithic artefacts and the surface sedimentary layer (considering that the samples have always been at or close to their sampling depth) as well as the deduced maximum uplift rate of ~170 m.Ma^{-1} are in agreement with the known tectonic evolution and the climatic variability of this area.

This study confirms the antiquity of the hominin presence in western Africa more than 2000 km away from the closest old hominin fossil sites.

1. Introduction

Although being the second largest country of the subsahelian Africa, Angola remains geologically and archeologically poorly characterized. During the 19th and the first part of the 20th centuries, geological studies were mainly dedicated to mineral resources. These early works, mentioned in the literature, are in Portuguese and are not widely available. The surveys nearly stopped because of the civil war lasting from 1960 to 2002. Despite the conflict has ended, numerous mined areas limit the surveys. Nonetheless, over the last quarter of century, archaeologic researches lead by a French-Angolan Team in the Benguela Province continue.

Studies carried out since 1993 in the Baia Farta region (Fig. 1) (southern Angola) by archaeologist Manuel Gutierrez highlighted the existence of ancient lithic, pre-Acheulean and Acheulean industries, in stratigraphy and over vast areas (Dungo area; [19,20]). The discovery, in Dungo V, a paleo-lagoon, of two sub-complete whale fossils with lithic tools intimately mixed with the bones, in an area presumed to be too acidic to produce and conserve fossils, gives importance to this area with regards to the history of the first hominins evolution in Africa.

* Corresponding author.
E-mail address: lebatard@cerege.fr (A.-E. Lebatard).
[1] Georges Aumaître, Karim Keddadouche.

https://doi.org/10.1016/j.nimb.2019.05.052
Received 18 December 2017; Received in revised form 20 May 2019; Accepted 20 May 2019
Available online 28 May 2019

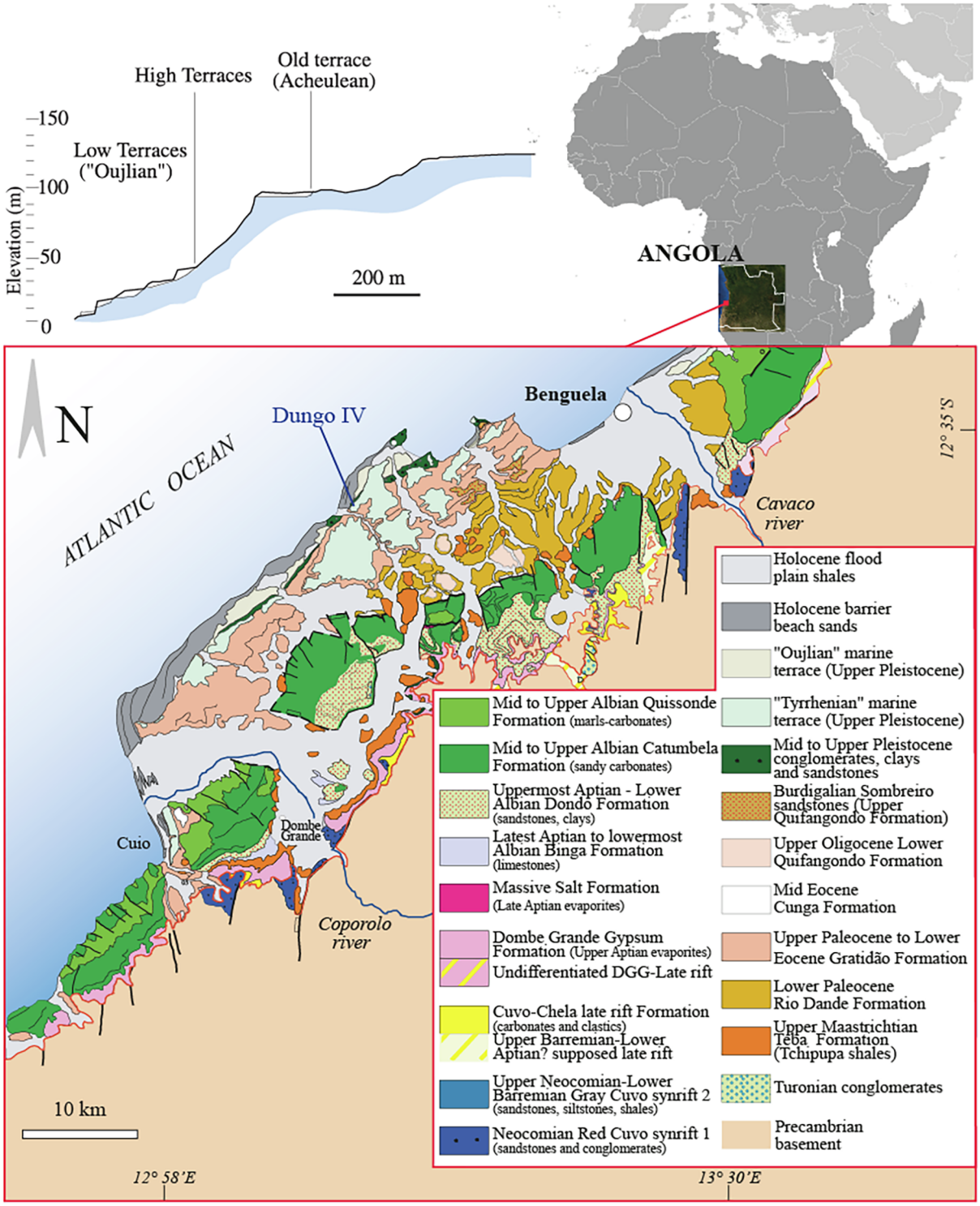

Fig. 1. The Dungo Palaeolithic area: Simplified geological map of the South Benguela Region and schematic topographical profile (modified from [18]).

Up to now the chronological succession of these industries is based on their relative stratigraphic positions. The presence of numerous artifacts on these sites has led to a search for a dating method adapted to the regional geological conditions where the absence of volcanism requires the use of dating methods able to overcome the chronological limits of the already tested Uranium / Thorium method [20]. Considering the configuration of the Dungo IV site, the cosmogenic nuclides burial dating method (the $^{26}Al/^{10}Be$ dating method) appears to be well-suited.

The development of dating methods based on cosmogenic nuclides for the dating of palaeoanthropological sites and, more broadly, for constraining the chronological framework of the Prehistoric periods in Africa has high added value. Relying only on the occurrence of quartz minerals, these methods may indeed reveal the importance for the understanding of the Paleolithic of areas that would have been nevertheless neglected. They could also allow comparing the Prehistory of southwestern Africa to the better known Prehistory of the East of the continent. At this point, it is worth noting that until the discoveries of

Abel and Toumaï, the history of mankind seemed to have taken place in the East of the continent.

The $^{26}Al/^{10}Be$ burial dating method has been successfully used over the last 15 years leading to an increasing interest of the archeologists of applying it at Pliocene and early Pleistocene sites to better understand the hominin evolution and diffusion.

In Africa, all the applications were concentrated in South Africa, especially in the Cradle of Humankind area. The first attempt was made at Sterkfontein where the $^{26}Al/^{10}Be$ burial dating method constrained the age of hominin remains at around 4 Ma [35]. This date was recently revised at 3.7 Ma using an improved $^{26}Al/^{10}Be$ burial dating method [17]. The earliest "Oldowan" stone tools from the site were dated at 2.2 Ma. In the nearby Swartkrans site, cosmogenic nuclides derived ages have demonstrated the presence of hominin over the time period comprised between 1 Ma and 2.2 Ma [12]. Using this same method, the age of the Rietputs Formation rich in Paleolithic artifacts was constrained near Windsorton between 1.2 and 1.9 Ma [11]. A hundred kilometers north from this last site, $^{26}Al/^{10}Be$ burial dating performed on the Oldowan deposit in the Wonderwerk cave imply a hominin occupation over the time period lasting from 1 Ma to 1.6 Ma [5]. Those four important sites are located ~2000 km SE from the Dungo area. The works carried out in Angola, and more particularly at the Dungo archaeological complexes at Baia Farta, show that the lithic industries are typologically similar to those found on sites of the East and the South of the continent. A first study performed in 2009 at Dungo IV provided preliminary mean burial duration for four pre-Acheulean stone tools [20]. Here, we present up-dated data for these same stone tools as well as data acquired along a depth-profile performed in the sedimentary layers deposited above them.

2. Studied area

2.1. Regional geological setting

The offshore area along the Angolan Atlantic margin, a part of the central segment of the south Atlantic margin, is divided in four basins: southwardly, the Lower Congo, the Kwanza (or Cuenza), the Benguela and the Namibia Basins [36].

Apart from a few geological studies, the coastal Quaternary formations of the Benguela Basin are poorly studied and the resulting observations (e.g. [30,18,26]) under-published because of confidentiality related to strategic and commercial interests. Earlier research conducted in this area was severely impeded by the civil war. More recently, geological research in Angola focused on the offshore and onshore Cretaceous deposits of the Kwanza Basin, north of the Baia Farta area and the Namibia Basin, rich in oil, (e.g. [21,36] and references therein; [46]).

The coastal zone of the Benguela Basin (Fig. 1) experiences a dry and arid desert climate punctuated by dramatic rains linked to the La Niña events, which sometimes produces fatal flooding. This zone is characterized by a narrow low-relief shore plain with planar surfaces rising in elevation eastward up to 145 m a.s.l. (Fig. 1) separated by escarpments of various altitude (e.g. [30,39,7]). The slightly tilted terraces consist of an abrasion surface covered mainly with a beach conglomerate. Giresse et al. [13] dated marine terraces in the area of Baia Farta and Lobito to the Upper Pleistocene period (Fig. 1) and interpreted them to be interglacial shorelines. Walker et al., [43] dated the 25 m a.s.l. terraces in the Benguela area at ~45 ka and extrapolated an age at ~80 ka for the 150 m a.s.l. terraces. This narrow coastal area is contiguous to a high-elevation escarpment (~2600 m a.s.l.) corresponding to the Great Escarpment described southward (along the Namibia and South Africa Atlantic coasts) and interpreted as a relic of an Early Cretaceous rift margin or as resulting from post-rifting processes [18] and references therein). The post-rifting sedimentation are characterized by the deposition, in the area of interest, of the Upper Paleocene-Lower Eocene Gratidão Formation alternating shales, siltstones and fine grained sandstones from a deltaic wedge. It is overlain by Upper to Middle Pleistocene deltaic clastic conglomerates and sandstones [18].

Quaternary raised marine terraces are widespread along the coast of Angola. Compared to the South and North Africa, the raised marine terraces of Angola remain poorly studied. The few studies performed in the Lobito-Benguela region highlight the local variability of Pleistocene shoreline elevation in response to lateral changes of the deformation rates, especially vertical uplift rates (e.g. [13,43]). These studies suggested that, in southern Angola, raised marine terraces did not reflect the chronological evolution of the Quaternary sea level changes. Therefore, the assumption was made that the still active rise may result from a combination of the marine fluctuations (e.g. [21,18,37]) and of tectonic processes, among which salt tectonic, affecting the Atlantic margin. Indeed, the effect on the deposits of the salt tectonic having been initiated during the Aptian-Albian period was studied in the Santa Clara area, south of the Dungo site [36].

2.2. Archaeological setting

For more than a century, archaeological discoveries attest to the long settlement history of the Angolan territory. However, the artefacts were mostly collected on surfaces close to research centers and the south-east of the country remained uninvestigated. To overcome this limitation, the National Archaeological Museum of Benguela initiated in the nineties in the framework of a French-Angolan collaboration studies in the area of the small town of Baia Farta. The Dungo area, known since the mid-twenty century for the presence of Acheulean lithic tools on 90–120 m a.s.l. paleobeach old terraces (e.g. [13]), was established as an archaeological educational site for Angolan and African academics. This allowed excavation of rich lithic assemblages at three main sites distributed along the Dungo wadi (7.6 km SW of Baia Farta; Fig. 2). At the Dungo IV site (12°40 S; 13°09 E; 104 m altitude; Figs. 2–3), two distinct archaeologic levels were discovered [20]. The upper, and therefore stratigraphically the youngest lithic tools level, is presumed to have been emplaced during the same time period than that of the Acheulean level in Baia Farta (e.g. [13]), which delivered bifaces and flakes produced by a local debitage. The lowest and therefore stratigraphically the oldest lithic tools level delivered numerous choppers technologically attributable to the pre-Acheulean time period. A kilometer eastward of the Dungo IV site, in a paleo-lagoon (Dungo V, Fig. 2, [19,20]), two sub-surface large whale fossils (*Balaenoptera* sp.) in anatomical connection were discovered in association with numerous lithic tools intimately mixed with the whale bones. The link between the hominins and the marine fauna is also demonstrated by the presence of oyster shells and other shellfishes mixed with the lithic tools [19]. The technology used to produce the lithic assemblage unearthed at the paleo-lagoon site (Dungo V) resembles to that used to produce the oldest lithic assemblage at the Dungo IV site. This is also the case at the Dungo XII site located on the left bank of the Dungo wadi, in the front of the Dungo IV site. In addition to casting doubt on the supposition that the soil pH is too acid in western Africa to preserve ancient bones, the Dungo V site provides the oldest evidence of stranded marine mammal scavenging by hominins in this part of Africa. In an attempt to absolutely date the oldest lithic assemblage, the overall configuration of the Dungo IV site appears the most relevant. A chronology of the site is our goal.

2.3. Dungo IV setting

At the archeological educational site, the edge of a 104 m a.s.l. terrace, on the right bank of the Dungo wadi (Fig. 2), surveyed since the 90's and on which 100 m2 exhibiting two distinct archaeological levels (Fig. 3) were unearthed, was selected to perform this study because of the lower thickness of the non-consolidated overlying deposit compared to the center of the terrace and for security reasons. Indeed, at the

Fig. 2. The Dungo Palaeolithic area, Benguela Region, Angola (Source: Image©2017 GoogleEarth) and panoramic view from the Dungo IV site (Photo©2014 AEL).

selected site, lithic artefacts appear to be spread on the top of a sand covered conglomerate. This paleobeach level, mapped as a Tyrrhenian marine terrace (Upper Pleistocene [18]; Fig. 1), corresponds to a cemented conglomerate covering an indurated white sandstone layer (Fig. 4; White Sandstone Paleobeach formation). This nearly planar marine terrace formation (old marine abrasion surface) is dissected by pluri-metric gullies, probably due to wave-action. The conglomerate is composed of cemented pebbles exhibiting various regional lithologies. Some oyster and other bivalve shells are visible at its top as well as along the gullies walls, which reinforce the marine origin for these layers. The rich lithic assemblage associated with the oldest archeological level mainly comprises choppers spread over the conglomerate surface, some being unearthed from the bottom of the gullies. The lithology of the tools and the pebbles from the conglomerate being similar, a local production of the tools is conceivable.

Above the paleobeach and in the gullies, the Red Sand formation (Figs. 3, 4) may reach more than 4 m thick at the center of the terrace. The material composing this Red Sand unit shows a graded bedding. From its summit (no soil) to the base are: a layer of fine grained red sand with scarce fine gravels (~40 cm); a fine gravelly red sand (~40 cm); a red sandy matrix fine gravel (~40 cm); and, finally, a red gravel to microconglomerate capping the paleo-morphology (greater than1 m thick). No bioturbation or aeolian markers were observed along this deposit at the studied site. The Acheulean layer was found at 120 cm depth. The red–orange color may indicate a laterization process, but no other formation can ascertain this assumption on the terrace. Despite the limited information available, the graded bedding observed in this formation suggests deltaic formation.

3. Materials, Methods, and results

3.1. Materials

The four pre-Acheulean quartzite stone tools were taken in 1996 at a depth of ~ 3 m in a gully (e.g. Fig. 3). They are denoted as MNAB Dungo4 9–7-96 NC-RAV-3n° 1389, MNAB Dungo4 9–7-96 NC-RAW-11n° 1397, MNAB Dungo4 9–7-96 NC-R-34n° 1420 and MNAB Dungo4 9–7-96 NC-R-40n° 1426 in the collections. In this study, these names are shortened to DUN-1389, DUN-1397, DUN-1420, and DUN-1426, respectively. Preliminary burial durations concerning these samples were published in Gutierrez et al. [20]. They were nevertheless reprocessed during this study from the quartz reserve following an improved chemical protocol.

In 2014, 29 samples have been taken at 15 different depths at the Dungo IV site, from the surface (Dungo4-14-3a and Dungo4-14-3b) down to 411 cm depth (Dungo4-14–15) (Figs. 3–4). Two samples were collected at each sampling depth, except at 411 cm (Dungo4-14–15), for the measurement of in situ-produced ^{10}Be and ^{26}Al concentrations

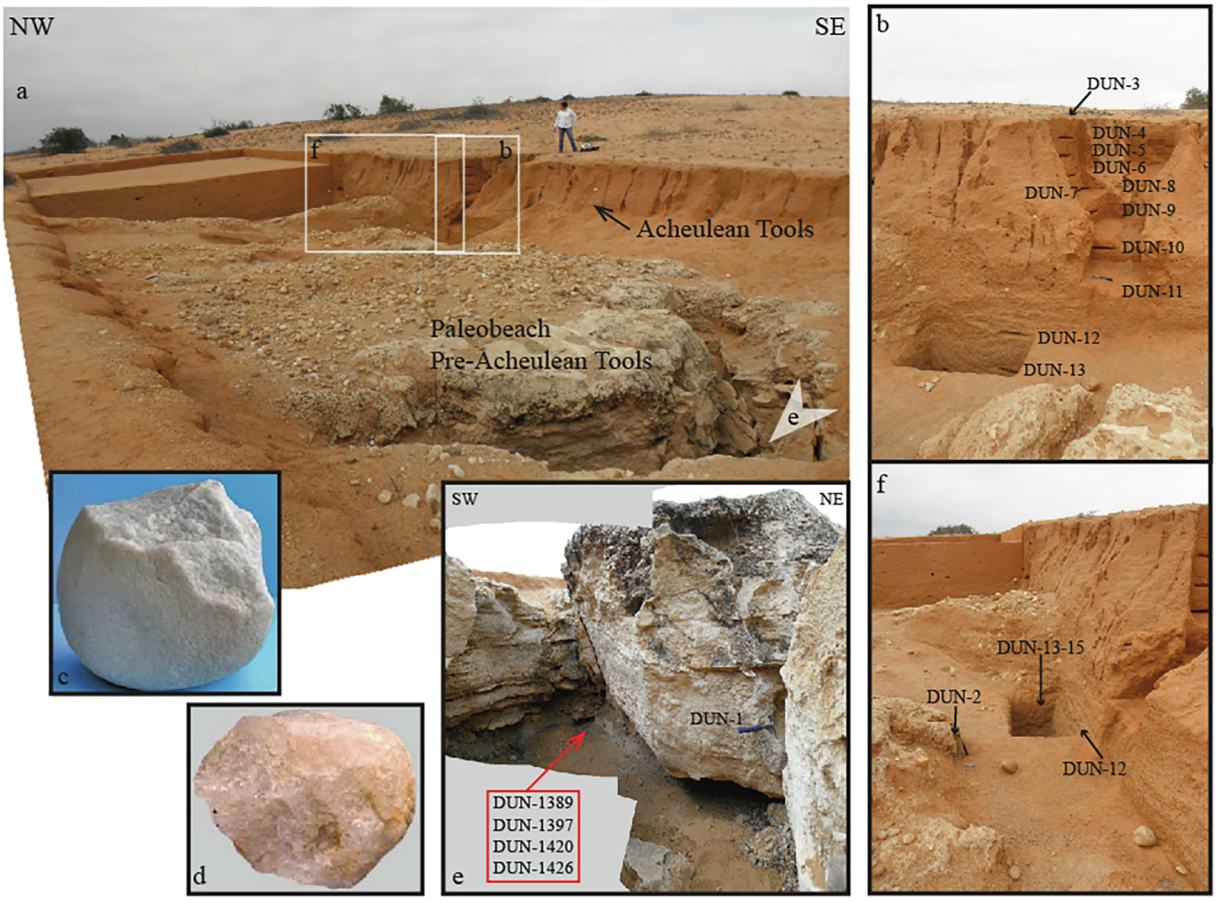

Fig. 3. The Dungo IV Palaeolithic site. Sampling and stone tools locations. b, e and f are zooms in relation to the panorama a (Photos©2014 AEL). c and d are two of the dated lithic tools (modified from [20]). For the sedimentary samples, DUN-1 to DUN-15, correspond in the Tables and text to Dungo4-14–1 to Dungo4-14–15. The stone tools ref., collected in 1996 by Manuel Gutierrez, are fully labellized in the Table 1 and here simplified in DUN-1389 for MNAB DUNGO 4 9–7-96 NC-RAV 3n° 1389, …

(Table 1). This sampling enables two depth-profiles, one along the Red Sand sedimentary unit covering, thanks to the gully, the entire 0 to 387 cm depth range, and one along the White Sandstone Paleobeach formation covering the 287 to 411 cm depth range. For the Red Sand unit depth-profile, 26 samples were collected at least every ~30 cm along the first ~2.3 m (Figs. 3–4, Table 1). The White Sandstone Paleobeach formation was sampled at three different depths, including one (Dungo4-14–1) in the gully, location of the studied stone tools, and one (Dungo4-14–15) at the base of the trench (Figs. 3–4, Table 1). The depth-profile along the Red Sand formation is expected to lead to an exponential decrease of the concentrations governed by the attenuation length of the cosmic-ray particles impinging since its deposition an unperturbed sedimentary layer under denudation, both the exposure duration and the denudation rate being then determinable. The trend of the depth-profile along the White Sandstone Paleobeach formation is similar to the one along the Red Sand unit that buried it. The ratio of two cosmogenic nuclides having significantly different half-lives allows then to determine, at least, the burial duration.

3.2. Methods

Based on the relative decay of the in situ-produced ^{26}Al and ^{10}Be cosmogenic nuclides, the ^{26}Al/^{10}Be burial dating method has benefited over the past 16 years of significant progress regarding both the understanding of its fundamental principles and of the processes of purification and separation of aluminum of the matrices studied as well as of technological developments enabling detection by AMS much more effective [8,28]. All these advances have contributed to extend its scope (e.g. [16]). Formed by nuclear reactions induced by the cosmic ray derived energetic particles on silicon (Si) and oxygen (O), ^{26}Al and ^{10}Be nuclides accumulate within the quartz (SiO_2) mineral fraction (in-situ production) of the rocks exposed at the Earth's crust surface with a known ^{26}Al/^{10}Be production ratio. The cosmic ray flux being efficiently attenuated by matter, burial below few meters of matter of previously exposed surfaces or artefacts leads to a sufficient reduction of the effective energetic particle flux to stop the ^{26}Al and ^{10}Be production. Both cosmogenic nuclide initial concentrations start to radioactively decay according to their respective half-life (^{26}Al: 0.705 ± 0.024 Ma [33,31]; ^{10}Be: 1.387 ± 0.012 Ma [22,6]), the ratio decreasing with an apparent half-life of 1.48 ± 0.04 Ma. The measurement of the latter allows a determination, when compared to the known initial ratio, of the burial duration of the studied sample over the time range 100 ka - ~5 Ma [15].

The physico-chemical treatments performed on the Angolan samples as well as the Accelerator Mass Spectrometry measurements at ASTER (CEREGE, Aix-en-Provence) of their ^{10}Be and ^{26}Al concentrations followed the protocols and parameters fully described in Lebatard et al. ([25] and references therein). The resulting ^{26}Al/^{10}Be ratio associated to each sample allows to determine their corresponding burial duration as well as the pre- and post-burial denudation rate they experienced using the modeling methodology fully described in the Supporting Online Material of Pappu et al. [34].

The surface ^{26}Al/^{10}Be spallogenic production rate ratio is 6.61 ± 0.52 due to the normalization of the measured ^{26}Al/^{27}Al ratios to the in-house standard SM-Al-11 whose ^{26}Al/^{27}Al ratio of $(7.401 \pm 0.064) \times 10^{-12}$ has been cross-calibrated [1] against primary standards from a round-robin exercise [27]. ^{10}Be/^{9}Be ratios were

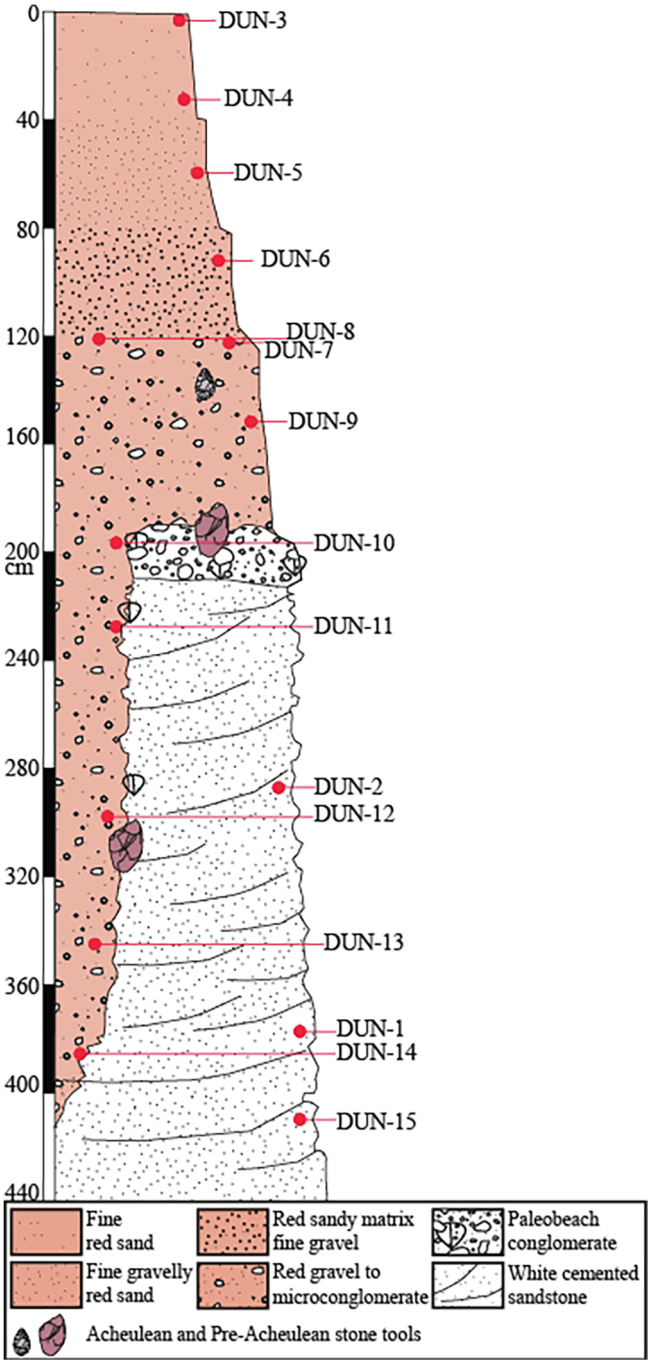

Fig. 4. Stratigraphic log of the Dungo IV Palaeolithic site and sampling locations. For the sedimentary samples, DUN-1 to DUN-15, correspond in the Tables and text to Dungo4-14–1 to Dungo4-14–15.

calibrated against NIST4325 with a corrected ratio of (2.79 ± 0.03) 10^{-11} [32]. The CosmoCalc Excel add-in [41] was used to scale the neutronic production rates according to the polynomial from Stone [40] based on a sea level and high latitude (SLHL) production rate of 4.03 ± 0.18 at g^{-1} a^{-1} [29,2]. The computing process relies on the parameters of Braucher et al. [3] for muon contributions.

The modeling of the ^{10}Be and ^{26}Al concentrations determined along the depth profiles allow quantifying minimum and maximum burial durations as well as before and after burial denudation rates [34,25]. A model based on the sole differential cosmogenic nuclide radioactive decay, that is assuming no post-burial production ("Model without post-burial production"), yields minimum burial durations and the associated before-burial denudation rates. This approach is equivalent to the graphical determinations in an exposure-burial diagram (^{26}Al/^{10}Be versus ^{10}Be graph; e.g. [14]), which aims to reproduce the minimum burial duration required to reach the determined ^{26}Al/^{10}Be from the initial one by the sole differential radioactive decay and for a given before-burial denudation rate. A second model assuming relatively stable environmental conditions since the burial and post-burial production ("Model with post-burial production") yields maximized burial durations and the associated before- and after-burial denudation rates.

Uncertainties associated with the ratios, the durations and the denudation rates, reported as 1σ, result from the propagation of the uncertainties of the different parameters and measurements used during the computing.

The measured values may, however, result from more complicated scenarios involving repeated burials and exposures which would obviously lead to significantly longer burial duration.

3.3. Results

Table 1 summarizes all the ^{10}Be and ^{26}Al measurements and the resulting ^{26}Al/^{10}Be ratios obtained for the 29 sediment samples and the 4 stone tools.

The concentration of the 24 samples taken along the surface Red Sand formation experiencing denudation should decrease exponentially according to the cosmic ray derived particles attenuation length and the effective denudation rate (e.g. [3]). However, as evidenced Fig. 5, both the calculated ^{10}Be and ^{26}Al concentrations and the resulting ratios of all these 24 sediment samples are not significantly different, whatever the depth considered. The test statistic proposed by Ward and Wilson [44] as well as the Kernel Density Estimation (KDE) standard statistical technique [42] performed on the ^{26}Al/^{10}Be ratios of the Red Sand formation samples demonstrates that they all belong to the same population. This is confirmed by the almost perfectly Gaussian distribution of the considered data centered on a single peak (Fig. 6a). The uncertainties associated to each sample being taken into account, the "Model without post-burial production" (Table 2) leads to a minimum weighted mean burial duration of 614.15 ± 9.50 ka and to pre-burial denudation rates ranging from 3.6 to 6.7 $m.Ma^{-1}$ leading to a before-burial weighted mean denudation rate of 4.5 $m.Ma^{-1}$. The "Model with post-burial production" leads to a maximum weighted mean burial duration of 662.05 ± 10.24 ka, not significantly different from the minimum one. Similarly, the calculated before-burial weighted mean denudation rate is fortunately not different from that calculated from the "Model without post-burial production". The after-burial denudation rate allowing to best fitting the data is 70.9 $m.Ma^{-1}$ (Table 2).

The ^{10}Be and ^{26}Al concentrations and the resulting ratios of the samples (n = 5) taken along the profile in the White Sandstone Paleobeach formation are again almost similar whatever the depth. The Ward and Wilson [44] statistic test as well as the standard statistical KDE technique performed on the ^{26}Al/^{10}Be ratios demonstrates that they all belong to the same population. This is also confirmed by the almost perfectly Gaussian distribution of the considered data centered on a single peak (Fig. 6b). More importantly, the "Model without post-burial production" and the "Model with post-burial production" (Table 2) lead to a minimum weighted mean burial duration of 617.15 ± 25.56 ka and a maximum weighted mean burial duration of 662.05 ± 27.42 ka, respectively, indistinguishable from those modeled from the Red Sand formation samples. The "Model without post-burial production" leads to pre-burial denudation rates ranging from 5.1 to 15.7 $m.Ma^{-1}$ leading to a before-burial weighted mean denudation rate of 8.5 $m.Ma^{-1}$. The after-burial denudation rate allowing to best fitting the data is equal to that applied to the Red Sand formation that is 70.9 $m.Ma^{-1}$ (Table 2).

These combined ^{10}Be and ^{26}Al measurements lead us to conclude that all the samples taken from both the Red Sand and the White Sandstone Paleobeach formations most probably belong to the same population, even if the concentration of both cosmogenic nuclides are

Table 1
^{10}Be, ^{26}Al concentrations and ^{26}Al/^{10}Be ratios results.

Unit	Sample		Depth (cm)			Depth (g.cm^{-2})	Dissolved quartz (g)	^{9}Be carrier (10^{19} at.)	^{27}Al carrier (10^{19} at.)	^{10}Be (10^{5} at.g^{-1})			^{26}Al (10^{5} at.g^{-1})			^{26}Al/^{10}Be		
Red Sand formation	Dungo4-14–3	a	2.5	±	2.5	6.5	19.585	2.040	0.0	3.601	±	0.121	17.177	±	0.785	4.770	±	0.270
		b	2.5	±	2.5	6.5	8.129	2.056	1.209	3.402	±	0.125	18.124	±	1.112	5.328	±	0.381
	Dungo4-14–4	a	32.5	±	2.5	84.5	19.097	2.058	0.0	3.441	±	0.115	16.616	±	0.825	4.829	±	0.289
		b	32.5	±	2.5	84.5	7.950	2.087	1.278	3.659	±	0.143	17.614	±	1.132	4.813	±	0.362
	Dungo4-14–5	a	59.5	±	2.5	154.7	15.760	2.042	0.016	3.405	±	0.112	16.345	±	0.715	4.801	±	0.263
		b	59.5	±	2.5	154.7	8.119	2.053	1.269	3.466	±	0.137	18.853	±	1.101	5.439	±	0.383
	Dungo4-14–6	a	91.5	±	2.5	237.9	19.607	2.052	0.0	3.263	±	0.108	17.158	±	0.716	5.259	±	0.280
		b	91.5	±	2.5	237.9	7.295	2.059	1.261	3.558	±	0.157	18.096	±	1.452	5.085	±	0.466
	Dungo4-14–8	a	119.5	±	2.5	312	18.920	2.043	0.0	3.280	±	0.108	16.490	±	0.718	5.027	±	0.274
		b	119.5	±	2.5	312	8.245	2.056	1.046	3.118	±	0.105	16.528	±	1.339	5.301	±	0.465
	Dungo4-14–7	a	120.0	±	2.0	310.7	18.853	2.043	0.0	3.480	±	0.114	16.987	±	0.702	4.881	±	0.258
		b	120.0	±	2.0	310.7	7.446	2.057	1.213	3.350	±	0.130	18.781	±	1.146	5.606	±	0.406
	Dungo4-14–9	a	152.0	±	3.0	395.2	18.930	2.038	0.0	3.085	±	0.101	14.740	±	0.769	4.778	±	0.294
		b	152.0	±	3.0	395.2	7.822	2.058	1.181	3.237	±	0.117	16.578	±	1.030	5.122	±	0.368
	Dungo4-14–10	a	202.5	±	2.5	526.5	20.138	2.045	0.0	3.125	±	0.108	15.295	±	0.847	4.894	±	0.319
		b	202.5	±	2.5	526.5	8.156	2.060	1.172	3.127	±	0.119	14.572	±	0.917	4.660	±	0.343
	Dungo4-14–11	a	231.0	±	1.0	600.6	19.331	2.043	0.0	3.290	±	0.116	16.220	±	0.694	4.930	±	0.273
		b	231.0	±	1.0	600.6	7.659	2.057	1.168	3.108	±	0.133	15.596	±	1.179	5.018	±	0.436
	Dungo4-14–12	a	297.5	±	2.5	773.5	19.352	2.053	0.0	2.700	±	0.096	12.355	±	0.549	4.576	±	0.261
		b	297.5	±	2.5	773.5	7.935	2.047	1.214	2.618	±	0.108	13.069	±	1.181	4.992	±	0.496
	Dungo4-14–13	a	346.0	±	4.0	899.6	19.232	2.039	0.0	2.361	±	0.079	11.669	±	0.559	4.941	±	0.288
		b	346.0	±	4.0	899.6	7.504	2.206	1.111	2.142	±	0.100	11.064	±	0.796	5.166	±	0.443
	Dungo4-14–14	a	385.0	±	5.0	1001	19.486	2.044	0.0	2.239	±	0.075	9.897	±	0.534	4.421	±	0.281
		b	385.0	±	5.0	1001	7.923	2.056	1.188	2.202	±	0.155	11.529	±	1.007	5.237	±	0.588
White Sandstone Paleobeach formation	Dungo4-14–2	a	287.0	±	3.0	746.2	19.195	2.049	0.0	1.847	±	0.065	8.300	±	0.837	4.495	±	0.480
		b	287.0	±	3.0	746.2	6.712	2.059	1.165	1.749	±	0.097	9.084	±	0.822	5.194	±	0.552
	Dungo4-14–1	a	377.0	±	3.0	980.2	19.483	2.048	0.0	2.561	±	0.087	13.130	±	0.592	5.126	±	0.290
		b	377.0	±	3.0	980.2	8.047	2.048	1.176	2.663	±	0.094	13.853	±	0.885	5.202	±	0.379
	Dungo4-14–15	a	411.0	±	4.0	1068.6	7.609	2.060	1.410	1.057	±	0.067	5.130	±	0.662	4.856	±	0.698
Tools	MNAB	a	300.0	±	–	780	40.023	2.034	0.0	5.458	±	0.176	19.029	±	0.634	3.486	±	0.161
	Dungo4 9–7-96 NC-RAV-3n° 1389	b	300.0	±	–	780	7.752	2.040	1.791	5.174	±	0.171	17.809	±	1.422	3.442	±	0.297
	MNAB	a	300.0	±	–	780	40.074	2.037	0.0	10.325	±	0.337	39.415	±	1.185	3.817	±	0.169
	Dungo4 9–7-96 NC-RAW-11n° 1397	b	300.0	±	–	780	7.518	2.053	1.933	10.861	±	0.351	40.591	±	1.427	3.737	±	0.178
	MNAB	a	300.0	±	–	780	40.008	2.035	0.0	6.033	±	0.173	12.681	±	0.393	2.102	±	0.089
	Dungo4 9–7-96 NC-R-34n° 1420	b	300.0	±	–	780	7.500	2.056	2.015	6.235	±	0.209	13.149	±	0.909	2.109	±	0.162
	MNAB	a	300.0	±	–	780	39.994	2.047	0.0	1.776	±	0.060	5.324	±	0.169	2.997	±	0.138
	Dungo4 9–7-96 NC-R-40n° 1426	b	300.0	±	–	780	7.924	2.049	1.824	1.848	±	0.097	5.473	±	1.445	2.961	±	0.797

^{26} Al/^{27}Al ratios were calibrated against SM-Al-11 standard with a ^{26}Al/^{27}Al ratio of (7.401 ± 0.064)0.10^{-12} [27] and ^{10}Be/^{9}Be ratios were calibrated against NIST4325 with a corrected ratio of (2.79 ± 0.03) 10^{-11} [32]. Uncertainties (± 1σ) include only analytical uncertainties. In the Table, the Tools-a data were obtained in 2009 [20]. The mean density of the Red Sand formation is 2.6 g.cm^{-3}. In each sample, addition of ~1 μl of the LN2C in-house phenakite 3.10^{-3} g.g^{-1} ^{9}Be carrier solution. ^{27}Al natural concentrations were measured by ICP-OES and a SCP commercial ^{27}Al carrier was added if the natural concentration was insufficient to perform a measurement. The 2009 tools-a measurements were corrected for the chemical blank ratios of 2.94 ± 0.58 10^{-15} and 5.61 ± 1.83 10^{-15} for ^{10}Be/^{9}Be and ^{26}Al/^{27}Al ratio, respectively. The 2015 profiles-a measurements were corrected for the chemical blank ratios of 2.49 ± 0.68 10^{-15} and 3.75 ± 3.75 10^{-15} for ^{10}Be/^{9}Be and ^{26}Al/^{27}Al ratio, respectively. The 2016 profiles-b and tools-b measurements were corrected for the chemical blank ratios of 3.01 ± 0.74 10^{-15} and 1.77 ± 0.31 10^{-14} for ^{10}Be/^{9}Be and ^{26}Al/^{27}Al ratio, respectively.

lower in the White Sandstone Paleobeach formation samples than in the Red Sand formation samples. This is most likely due to different exposure durations at the surface before their emplacement within their respective unit. Performing the Ward and Wilson [44] statistic test as well as the standard statistical KDE technique on the ^{26}Al/^{10}Be ratios of all the then considered 29 samples confirms that they indeed all belong to the same population (Fig. 6c). The "Model without post-burial production" and the "Model with post-burial production" lead to a minimum weighted mean burial duration of 614.52 ± 8.91 ka and a maximum weighted mean burial duration of 662.05 ± 9.60 ka, respectively, once again indistinguishable from those modeled from the Red Sand and the White Sandstone Paleobeach formation samples.

For the four pre-Acheulean quartzite stone tools, the preliminary data obtained in 2009 (*tools*-a in Tables 1 and 2; [20]) were revised using the most recently re-evaluated physical parameters constraining the cosmogenic nuclides production and new ^{10}Be and ^{26}Al concentration measurements (*tools*-b in Tables 1 and 2). The "Model without post-burial production" leads to (Table 2) a minimized burial duration of 0.74 Ma, that is the obtained minimum weighted mean burial duration minus its uncertainty (0.77–0.03 Ma) (MNAB Dungo4 9–7-96 NC-RAW-11n° 1397, Table 2). The "Model with post-burial production" leads to a maximized burial duration of 2.11 Ma that is the obtained maximum weighted mean burial duration plus its uncertainty (2.02 + 0.09 Ma) (MNAB Dungo4 9–7-96 NC-R-34n° 1420, Table 2). The studied tools come from a depression in the indurated paleo-beach, which may be a zone of accumulation of artefacts coming from different

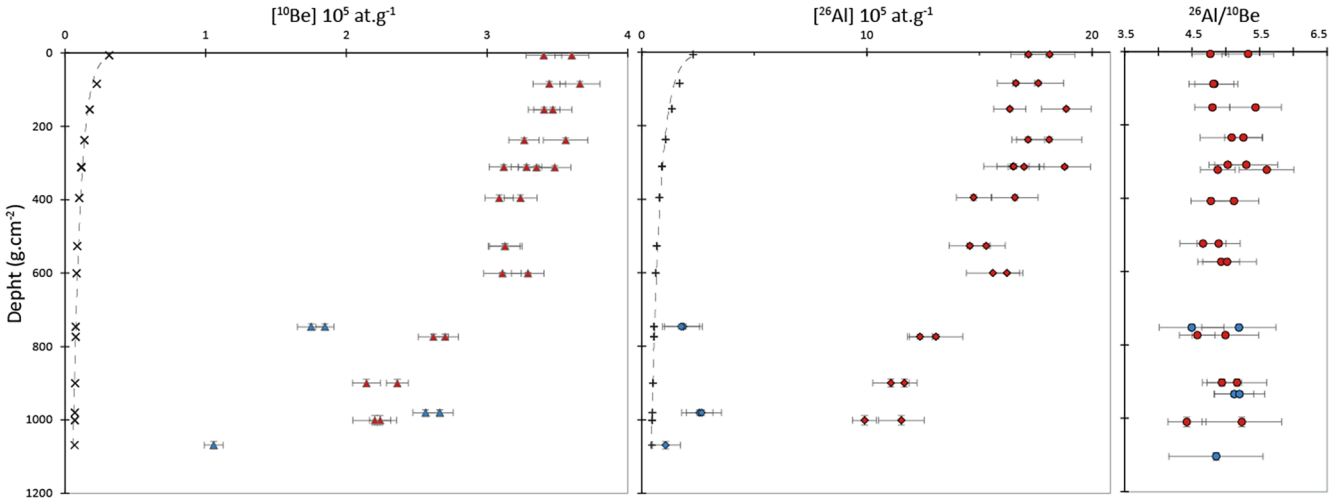

Fig. 5. ^{10}Be and ^{26}Al concentrations and ^{26}Al/^{10}Be ratio along the depth profiles. The 29 ^{26}Al/^{10}Be ratios of the sediment samples are considered as a unique population according to the statistical treatment (Fig. 6C). The red marks represent the data for the Red Sand formation, and the blue marks those for the White Sandstone Paleobeach formation. Triangle, diamond and dots respectively correspond to ^{10}Be concentrations, ^{26}Al concentrations, and ^{26}Al/^{10}Be ratios. Dark curves and marks correspond to both ^{10}Be and ^{26}Al post-production concentrations accumulated in the samples since the deposition of the Red Sand formation (Cf. Table 2). (For interpretation of the references to color in this figure legend, the reader is referred to the web version of this article.)

depths of the latter. The sampling conditions may thus be one possible explanation for the dispersion of the obtained burial durations. It can also be hypothesized that the tools were produced from raw material collected in a previously buried conglomerate. However, the pre-depositional denudation rates associated to each stone tool are significantly different and range from 0.74 m.Ma^{-1} to 4.50 m.Ma^{-1}. This suggests different origins for the rocks the tools are made of and implies either that the hominins collected their raw material at different sources (possibly, previously buried conglomerates) or that the studied artifacts were reworked from older and higher gravel deposits. In any case, the post-burial denudation rate of 70.5 m.Ma^{-1} derived from the stone tools combined ^{10}Be and ^{26}Al concentrations is similar to the value computed for the overlying material, i.e. the Red Sand and the White Sandstone Paleobeach formations, validating their concomitant evolution since their emplacement.

4. Discussion-Conclusion

Considering that the samples have always been at the depth at which they were collected, the best fit between the modeled and measured concentrations leads to a minimum weighted mean burial duration of 614.15 ± 9.50 ka and a maximum weighted mean burial duration of 662.05 ± 10.24 ka for the Red Sand formation.

Although there is no evidence that the surface was recently truncated, except perhaps the increasing presence of the red sand layer further from the coast, which may indicate a formerly thicker sand layer, the best fit as a function of depth of the measured ^{10}Be and ^{26}Al concentrations lead to a characteristic muonic attenuation length of ~1700 g.cm^{-2} and ~1500 g.cm^{-2}, respectively. This may result from a "recent" truncation of a thickness of an overlying deposit.

Considering that the current Red Sand Formation has been truncated, burial durations ranging from 585 ka to 786 ka and truncations lower than 4 m result from the modeling of the evolution of the ^{10}Be and ^{26}Al concentrations as a function of depth, the best fit in this case being a burial duration of 724 ka associated with a truncation of 3.4 m.

However, it is worth noting that considering a possible truncation or not do not significantly affect the deduced burial durations. This is in agreement with the outputs of the modeling, particularly the fact that low pre-burial denudation rates indicate that the materials (sediments and tools) most likely originated from a stable surface on which they accumulated large in situ-produced ^{10}Be and ^{26}Al concentrations whose upper limits correspond to the related steady-state equilibrium concentrations. This implies that the deposited material has a large inherited component. This hypothesis is supported by a study of Garzanti et al., [10] performed on numerous rivers from Angola. In this study, the origin of the material transported by the active rivers bracketing the Dungo area (i.e. Coprolo (S) and Catumbela (N) rivers) is 2 Ga old gabbroic rocks.

The consequence of such a scenario is that the in situ-produced ^{10}Be and ^{26}Al concentrations accumulated all along the thickness of the surface sedimentary layer since it has been deposited is almost negligible compared to the inherited in situ-produced ^{10}Be and ^{26}Al concentrations (less than 9% for the ^{10}Be and 13% for the ^{26}Al; Table 2, dark curves in Fig. 5). The temporal evolution of the in situ-produced ^{10}Be and ^{26}Al concentrations along the depth-profile (Fig. 5) is almost entirely controlled by the respective radioactive decay of both cosmogenic nuclides. Although this is not strictly burial, the significantly different ^{10}Be and ^{26}Al radioactive decay constants must imply that the ^{26}Al/^{10}Be ratio all along the profile evolves from an initial ^{26}Al/^{10}Be production ratio acquired by the sediments while at the surface to a constant lower value, whatever the depth, depending on the time elapsed since it has been deposited in the sedimentary layer. As previously presented and seen in Fig. 6c and Table 1, this is indeed the case. The Red Sand and White Sandstone Paleobeach formations record the same burial history. The hominin occupation surface (the paleobeach) was deeply covered by the Red Sand formation at least 614 ka ago and then subjected to a maximum denudation rate of 70.9 m.Ma^{-1} (Table 2).

On Fig. 1, the Dungo area surface is attributed to the Tyrrhenian (260–11 ka). However, located at an elevation of ~ 100 m and the surface Red Sand formation having been deposited at least 614 ka ago, it relates more to Middle Pleistocene period (MIS 15 or 16). This implies that the Dungo terrace is significantly older than previously thought. This unit may then be related to the braid-delta sequence of the Quelo (or Muceque) formation also observed northward in the Luanda region [38,4,45]. This Quelo formation is widely distributed in the surroundings of Luanda and is recorded as far as ~270 km N from the Dungo area (Kwanza River; [45]). However, the lack of stratigraphical constraints and markers in both areas makes correlations difficult. If the Dungo Red Sand is part of the Pleistocene deltaic Quelo formation, it was deposited during a major stage of relative sea level rise ([4] and references therein). The minimum age of 614 ka also post-dates the old

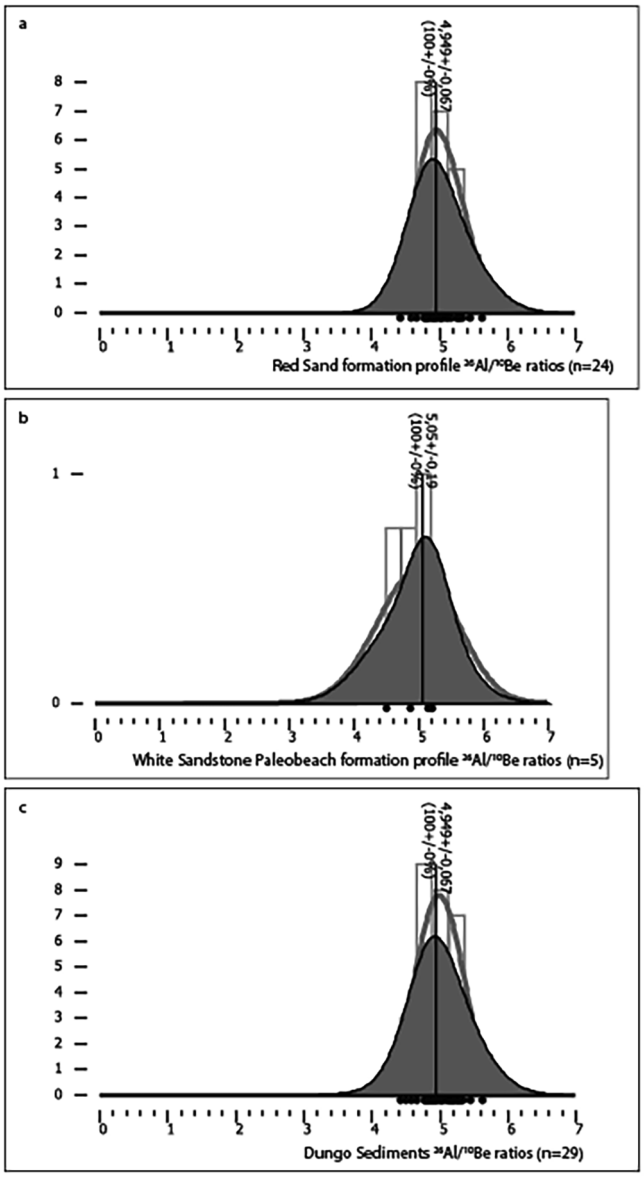

Fig. 6. Density Plots obtained using DensityPlotter 1.3 [42] presenting $^{26}Al/^{10}Be$ ratios for the two profiles separetly (a and b) and combined (c) for the Dungo IV site. a = the Red Sand formation profile (n = 24); b = the White Sandstone Paleobeach formation profile (n = 5); c = all sediments $^{26}Al/^{10}Be$ ratios at the Dungo IV site (n = 29). The central value can be related to the weighted mean value. The grey bold curve correspond to the Kernel Density Estimate curve, the grey peak correspond to the probability density curve. The black dots represent each sample $^{26}Al/^{10}Be$ ratio.

marine abrasion surface which was occupied by old hominins (i.e. the White Sandstone Paleobeach formation).

Furthermore, the current elevation of the paleobeach at 104 m a.s.l. allows an estimation of the Dungo area mean uplift rate. The burial duration of the White Sandstone Paleobeach and the Red Sand formations (between 614 and 662 ka) lead to a mean coastal uplift rate of ~ 165 $m.Ma^{-1}$. Integrated over the considered time period, this mean uplift rate is lower than the moderate minimum coastal uplift rate determined by Gallagher et al. [9] and Guiraud et al. [18] for the so-called "Old Terrace (Acheulean)" level (Fig. 1), that is ~ 400 $m.Ma^{-1}$, and for the Tyrrhenian terraces (250–310 $m.Ma^{-1}$), but one order of magnitude larger than the Cretaceous-Cenozoic uplift rate (15–30 $m.Ma^{-1}$). The current uplift rate for the region is ~ 2200 $m.Ma^{-1}$ (e.g. [43]).

The minimum burial duration of the tools of 0.74 Ma is significantly different from the maximum overlying material burial duration of 0.66 Ma, leaving the possibility of a different history for the four stone tools than for the sediments. The pre-burial denudation rates associated to the tools are much lower than those associated to the sedimentary formations. Several scenarios could explain such differences. The debitage chains evidenced on the beach surface [20] allows specifying the scenarios already discussed while presenting the results. These chains may indeed indicate that the hominins have brought on the paleobeach during a given period of time, but from diverse conglomeratic deposits common in the surroundings, the material from which the four tools found in the gully is made of, or have brought it at different periods extending since the Early to the Mid-Pleistocene (between ~ 2 and 0.7 Ma), indicating therefore that the site was occupied over a large time period. Such scenarios may be supported by the presence of stone tools at the Dungo V site where no pebbles deposits were available, indicating the transportation of artefacts in the paleo-lagoon by the hominins. Such scenarios take into account the fact that both the Red Sand and White Sandstone Paleobeach formations record the same burial history. This indeed implies that there is no possibility for scenarios involving multiple exposure-burial episodes of the paleobeach before the Red Sand formation deposition

The analyzed four quartzite pre-Acheulean lithic artefacts leading to burial durations ranging from 0.7 and 2 Ma at the Dungo IV site is contemporary of sites in South Africa dated using the same method. Indeed, ~ 2000 km SE from the Dungo area, in the center of South Africa, two sites have delivered stone artifacts characterized as Oldowan (between 1 and 1.6 Ma) at the Wonderwerk cave [5], and as early Acheulean (1.2 to 1.6 Ma) in the Reitputs Formation (Windsorton) [11,24,23]. Further SE, in the "Cradle of Humankind" World Heritage area, in the Sterkfontein cave, the earliest stone tools dated at around 2.2 Ma were related to the Oldowan period [17], and at Swartkrans the site occupation lasted between 1 and 2.2 Ma [12]. During the time period covered by the Dungo IV stone tools, that is between 0.7 and 2 Ma, in South Africa the presence of at least 3 hominin species, *Paranthropus robustus* and the early Homo (*Homo habilis* and *Homo ergaster*), is attested in the area. Despite the lack of hominin fossils in Angola, the convergence of the ages with the South African sites is remarkable. Pre- or early-Acheulean large stone tool appearance simultaneously in different areas of Africa involves a fast spread of the stone tool technology, but the scarce dated sites in the southern half of the African continent limit the global comprehension of the hominin Plio-Pleistocene dispersion. This nevertheless reinforces the remark of Gibbon et al., [11]: "The simultaneous appearance of the Acheulean in different parts of the continent implies relatively rapid technology development and the widespread use of large cutting tools in the African continent by ca 1.6 Ma."

Acknowledgments

This research was supported by the French Ministry for Foreign Affairs. The authors thank L. Léanni for her valuable assistance during chemical treatments and ICP-OES measurements. The ^{10}Be and ^{26}Al measurements were performed at the ASTER AMS national facility (CEREGE, Aix-en-Provence) which is supported by the INSU/CNRS, the ANR through the "Projets thématiques d'excellence" program for the "Equipements d'excellence" ASTER-CEREGE action, IRD. We thank the Benguela Archeological Museum, the Katyavalla Bwila University and the French-Angolan Archeological Research team for their support during the 2014 summer field mission. Prof. Michel Guiraud from the « Biogéosciences » unit of the « Université de Bourgogne » at Dijon (France) is also thanked for his help regarding the understanding of the regional geological evolution. The two reviewers, D.G. and an anonymous are thanked for open discussions, fair and constructive comments.

Table 2
Burial durations and denudation rates resulting from the model outputs.

Unit	Sample		Model Without Post-B production				Model With Post-B. production						
			Denud. before burial (m.Ma^{-1})	Min Burial duration (ka)			Denud. before B. (m.Ma^{-1})	Max Burial duration (ka)			Denud. after B. (m.Ma^{-1})	% [^{10}Be] Post-B.	% [^{26}Al] Post-B.
Red Sand formation	Dungo4-14–3	a	3.7	614.15	±	40.96	4.0	662.05	±	44.15	70.9	8.7	13.3
		b	3.8	614.15	±	48.97	4.1	662.05	±	52.79	70.9	9.2	12.6
	Dungo4-14–4	a	3.8	614.15	±	42.64	4.1	662.05	±	45.97	70.9	6.5	10.1
		b	3.6	614.15	±	50.97	3.8	662.05	±	54.94	70.9	6.2	9.6
	Dungo4-14–5	a	3.9	614.15	±	39.92	4.1	662.05	±	43.03	70.9	5.1	8.1
		b	3.7	614.15	±	48.37	3.8	662.05	±	52.14	70.9	5.0	7.1
	Dungo4-14–6	a	4.0	614.15	±	39.14	4.0	662.05	±	42.19	70.9	4.2	6.2
		b	3.6	614.15	±	60.26	3.7	662.05	±	64.96	70.9	3.9	5.9
	Dungo4-14–8	a	4.0	614.15	±	39.81	4.1	662.05	±	42.92	70.9	3.5	5.5
		b	4.2	614.15	±	58.01	4.3	662.05	±	62.53	70.9	3.7	5.5
	Dungo4-14–7	a	3.8	614.15	±	38.96	3.8	662.05	±	42.00	70.9	3.3	5.3
		b	3.8	614.15	±	49.40	3.8	662.05	±	53.25	70.9	3.5	4.8
	Dungo4-14–9	a	4.4	614.15	±	43.55	4.4	662.05	±	46.94	70.9	3.3	5.3
		b	4.1	614.15	±	49.11	4.1	662.05	±	52.94	70.9	3.1	4.7
	Dungo4-14–10	a	4.3	614.15	±	45.49	4.3	662.05	±	49.04	70.9	2.8	4.3
		b	4.4	614.15	±	50.07	4.4	662.05	±	53.98	70.9	2.8	4.5
	Dungo4-14–11	a	4.0	614.15	±	40.29	4.0	662.05	±	43.44	70.9	2.5	3.8
		b	4.3	614.15	±	57.57	4.3	662.05	±	62.06	70.9	2.6	3.9
	Dungo4-14–12	a	5.3	614.15	±	41.12	5.3	662.05	±	44.33	70.9	2.8	4.4
		b	5.3	614.15	±	64.69	5.3	662.05	±	69.73	70.9	2.9	4.1
	Dungo4-14–13	a	6.0	614.15	±	41.84	6.0	662.05	±	45.10	70.9	3.0	4.2
		b	6.6	614.15	±	56.88	6.7	662.05	±	61.31	70.9	3.3	4.5
	Dungo4-14–14	a	6.6	614.15	±	44.57	6.7	662.05	±	48.05	70.9	3.1	4.7
		b	6.3	614.15	±	72.29	6.4	662.05	±	77.93	70.9	3.1	4.0
White Sandstone Paleobeach formation	Dungo4-14–2	a	8.0	617.15	±	69.37	8.2	662.05	±	74.42	70.9	4.1	6.6
		b	8.3	617.15	±	69.04	8.5	662.05	±	74.06	70.9	4.3	6.0
	Dungo4-14–1	a	5.3	617.15	±	41.09	5.3	662.05	±	44.07	70.9	2.7	3.6
		b	5.1	617.15	±	49.96	5.1	662.05	±	53.59	70.9	2.6	3.4
	Dungo4-14–15	b	14.9	617.15	±	91.33	15.7	662.05	±	97.98	70.9	6.4	8.7
Tools	MNAB Dungo4 9–7-96 NC-RAV-3n° 1389	a	1.6	1132.00	±	65.80	1.6	1161.86	±	67.54	70.5	1.4	2.8
		b	1.7	1169.86	±	109.12	1.7	1202.10	±	112.12	70.5	1.5	3.0
	MNAB Dungo4 9–7-96 NC-RAW-11n° 1397	a	0.9	761.98	±	43.11	0.9	775.49	±	43.87	70.5	0.7	1.4
		b	0.8	777.53	±	46.08	0.8	790.84	±	46.87	70.5	0.7	1.3
	MNAB Dungo4 9–7-96 NC-R-34n° 1420	a	0.8	1965.27	±	107.93	0.8	2021.26	±	111.00	70.5	1.3	4.3
		b	0.8	1946.52	±	164.47	0.7	2000.32	±	169.01	70.5	1.3	4.1
	MNAB Dungo4 9–7-96 NC-R-40n° 1426	a	4.5	1656.36	±	96.12	4.4	1782.50	±	103.44	70.5	4.4	10.2
		b	4.3	1672.86	±	454.19	4.2	1796.04	±	487.63	70.5	4.2	9.9

In the Table, the Tools-a data were obtained in 2009 [20], and revised using the up-to-date parameters. The data were obtained using a Monte Carlo Regression Model (e.g.: [3,34]). The burial durations are in ka (1000 a). Burial age and denudation rate uncertainties (reported as 1σ) propagate the half-life uncertainties. The denudation rates are given in m.Ma^{-1} (meter per million years). Parameters used for the calculation: Latitude: 12.67°; Altitude: 104 m; Pressure: 1000.82 mbar; mean density: 2.6 g.cm^{-3}; Stone Scaling: 0.67; τ^{10}Be: 1.387 ± 0.0120 Ma [6,22], τ^{26}Al: 0.705 ± 0.024 Ma [33,31]; P10 SLHL: 4.03 ± 0.18 at.g^{-1}.a^{-1} [29,2], ^{10}Be sea level slow muon-induced production: 0.013 ± 0.012 at.g^{-1}.a^{-1}; sea level fast muon induced production: 0.040 ± 0.004 at.g^{-1}.a^{-1}; ^{26}Al sea level slow muon-induced production: 0.84 ± 0.017 at.g^{-1}.a^{-1}; ^{10}Be sea level fast muon-induced production: 0.081 ± 0.051 at.g^{-1}.a^{-1}; ^{26}Al/^{10}Be spallogenic production ratio: 6.61 ± 0.52; Att (Attenuation) Length neutrons: 160 g.cm^{-2}; Att Length slow muons: 1500 g.cm^{-2}; Att Length fast muons: 4320 g.cm^{-2} [3]. The studied site scaled neutronic production is 2.69 at.g^{-1}.a^{-1} for ^{10}Be and 17.82 at.g^{-1}.a^{-1} for ^{26}Al, slow muons production is 0.01 at.g^{-1}.a^{-1} for ^{10}Be and 0.88 at.g^{-1}.a^{-1} for ^{26}Al, and fast muons production is 0.04 at.g^{-1}.a^{-1} for ^{10}Be and 0.08 at.g^{-1}.a^{-1} for ^{26}Al [40,3]. B. = burial; Denud. = denudation; Min = minimum; Max = maximum. According to [34], the "Model without post-burial production" assuming that no cosmogenic nuclides were accumulated in the samples while buried (infinite burial depth) yields minimum burial duration. The "Model with post-burial production" assuming for modeling that the samples remained buried at their sampling depths and accumulated cosmogenic nuclides produced by muons yields maximized burial durations in a steady denudation over the burial period.

References

[1] M. Arnold, S. Merchel, D.L. Bourlès, R. Braucher, L. Benedetti, R.C. Finkel, G. Aumaître, A. Gottdang, M. Klein, The French accelerator mass spectrometry facility ASTER: improved performance and developments, Nucl. Inst. Meth. Phys. Res. B 268 (2010) 1954–1959.

[2] B. Borchers, S. Marrero, G. Balco, M. Caffee, B. Goehring, N. Lifton, K. Nishiizumi, F. Phillips, J. Schaefer, J. Stone, Geological calibration of spallation production rates in the CRONUS-Earth project, Quat. Geochronol. 31 (2016) 188–198.

[3] R. Braucher, S. Merchel, J. Borgomano, D.L. Bourlès, Production of cosmogenic radionuclides at great depth: a multi element approach, Earth Planet. Sc. Lett. 309 (1) (2011) 1–9.

[4] C. Cauxeiro, J. Durand, M. Lopez, Stratigraphic architecture and forcing processes of the late Neogene Miradouro da Lua sedimentary prism, Cuanza Basin, Angola, J. Afr. Earth Sc. 95 (2014) 77–92.

[5] M.D. Chazan, D.M. Avery, M.K. Bamford, F. Berna, J. Brink, Y. Fernandez-Jalvo, P. Goldberg, S. Holt, A. Matmon, N. Porat, H. Ron, L. Rossouw, L. Scott, L.K. Horwitz, The Oldowan horizon in Wonderwerk Cave (South Africa): archaeological, geological, paleontological, and paleoclimatic evidence, J. Hum. Evol. 63 (2012) 859–866.

[6] J. Chmeleff, F. von Blanckenburg, K. Kossert, D. Jackob, Determination of the ^{10}Be half-life by multicollector ICP-MS and liquid scintillation counting, Nucl. Inst. Meth. B 268 (2) (2010) 192–199.

[7] P.A. Dinis, J. Huvi, J. Cascalho, E. Garzanti, P. Vermeesch, P. Callapez, Sand-spits systems from Benguela region (SW Angola). An analysis of sediment sources and dispersal from textural and compositional data, J. Afr. Earth Sc. 117 (2016) 171–182.

[8] L.K. Fifield, S.G. Tims, C.R. Morton, L.G. Gladkis, ^{26}Al measurements with ^{10}Be

counting statistics, Nucl. Inst. Meth. B 259 (2007) 178–183.
[9] K. Gallagher, R. Brown, The Mesozoic denudation history of the Atlantic margins of southern Africa and southeast Brazil and the relationship to offshore sedimentation, in: N.R. Cameron, R.H. Bate, V.S. Clure (Eds.), The Oil and Gas Habitats of the South Atlantic, vol. 153, Geological Society, London, Special Publications, 1999, pp. 41–53.
[10] E. Garzanti, P. Dinis, P. Vermeesch, S. Andò, A. Hahn, J. Huvi, M. Limonta, M. Padoan, A. Resenti, M. Rittner, G. Vezzoli, Dynamic uplift, recycling, and climate control on the petrology of passive-margin sand (Angola), Sed. Geol. 375 (2018) 86–104.
[11] R.J. Gibbon, D.E. Granger, K. Kuman, T.C. Partridge, Early Acheulean technology in the Rietputs Formation, South Africa, dated with cosmogenic nuclides, J. Hum. Evol. 56 (2009) 152–160.
[12] R.J. Gibbon, T.R. Pickering, M.B. Sutton, J.L. Heaton, K. Kuman, R.J. Clarke, C.K. Brain, D.E. Granger, Cosmogenic nuclide burial dating of hominin-bearing Pleistocene cave deposits at Swartkrans, South Africa, Quat. Geochronol. 24 (2014) 10–15.
[13] P. Giresse, C.-T. Hoang, G. Kouyoumontzakis, Analyis of vertical movments deduced from a geochronological study of marine Pleistocene deposits, southern coast of Angola, J. Afr. Earth Sc. 2 (2) (1984) 177–187.
[14] D.E. Granger, A review of burial dating methods using 26Al and 10Be. Geological Society of America, special paper 415, Edited by Lionel L. Siame, Didier L. Bourlès, and Erik T. Brown, 2006, 1–16.
[15] D.E. Granger, P.F. Muzikar, Dating sediment burial with in situ-produced cosmogenic nuclides: theory, techniques, and limitations, Earth Planet. Sci. Lett. 188 (2001) 269–281.
[16] D.E. Granger, N.A. Lifton, J.K. Willenbring, A cosmic trip: 25 years of cosmogenic nuclides in geology, Geol. Soc. Am. Bull. 125 (9–10) (2013) 1379–1402.
[17] D.E. Granger, R.J. Gibbon, K. Kuman, R.J. Clarke, L. Bruxelles, M.W. Caffee, New cosmogenic burial ages for Sterkfontein Member 2 *Australopithecus* and Member 5 Oldowan, Nature 522 (2015) 85–88.
[18] M. Guiraud, A. Buta-Neto, D. Quesne, Segmentation and differential post-rift uplift at the *Angola* margin as recorded by the transform-rifted Benguela and oblique-to-orthogonal-rifted Kwanza basins, Mar. Pet. Geol. 27 (5) (2010) 1040–1068.
[19] M. Gutierrez, C. Guérin, M. Lénac, M. Piedade da Jesus, Exploitation d'un grand cétacé au Paléolithique ancien : le site de Dungo V à Baia Farta (Benguela, Angola), C. R. Acad Sci. Paris, Sciences de la Terre et des planètes / Earth and Planetary Sciences 332 (2001) 357–362.
[20] M. Gutierrez, C. Guérin, C. Karlin, M. da Piedade de Jésus, M.H. Benjamim, A.-E. Lebatard, D.L. Bourlès, R. Braucher, L. Leanni, Recherches archéologiques à Dungo (Angola). Un site de charronnage de baleine de plus d'un million d'années, Afrique: Archéologie & Arts 6 (2010) 25–47.
[21] M.P.A. Jackson, M.R. Hudec, K.A. Hegarty, The great West African Tertiary coastal uplift: fact or fiction? A perspective from the Angolan divergent margin, Tectonics 24 (2005) 278–302.
[22] G. Korschinek, A. Bergmaier, T. Faestermann, U.C. Gerstmann, K. Knie, G. Rugel, A. Wallner, I. Dillmann, G. Dollinger, Lierse von Gosstomski, Ch., Kossert K., Maiti M., Poutivtsev M., Remmert A., A new value for the ^{10}Be half-life by Heavy-Ion Elastic Recoil detection and liquid scintillation counting, Nucl. Inst. Meth. B 268 (2) (2010) 187–191.
[23] K. Kuman, R.J. Gibbon, The Rietputs 15 site and the Early Acheulean in South Africa, Quaternary Int. 480 (2018) 4–15.
[24] G.M. Leader, K. Kuman, R.J. Gibbon, D.E. Granger, Early Acheulean organized core knapping strategies ca. 1.3 Ma at Rietputs 15, Northern Cape Province, South Africa, Quaternary Int. 480 (2018) 16–28.
[25] A.-E. Lebatard, M.C. Alçiçek, P. Rochette, S. Khatib, A. Vialet, N. Boulbes, D.L. Bourlès, F. Demory, G. Guipert, S. Mayda, V.V. Titov, L. Vidal, H. De Lumley, Dating the Homo erectus bearing travertine from Kocabas, (Denizli, Turkey) at at least 1.1 Ma, Earth Planet. Sci. Let. 390 (2014) 8–18.
[26] P. Masse, O. Laurent, Geological exploration of *Angola* from Sumbe to Namibe: A review at the frontier between geology, natural resources and the history of geology, Comptes Rendus Geoscience 348 (1) (2016) 80–88.
[27] S. Merchel, W. Bremser, First international ^{26}Al interlaboratory comparison-Part I, Nucl. Inst. Meth. B 223–224 (2004) 393–400.
[28] K.-U. Miltenberger, A.M. Müller, M. Suter, H.-A. Synal, C. Vockenhuber, Accelerator mass spectrometry of ^{26}Al at 6 MV using AlO^- ions and a gas-filled magnet, Nucl. Inst. Meth. B 406 (2017) 272–277.
[29] S. Molliex, L.L. Siame, D.L. Bourlès, O. Bellier, R. Braucher, G. Clauzon, Quaternary evolution of a large alluvial fan in a periglacial setting (Crau Plain, SE France) constrained by terrestrial cosmogenic nuclide (^{10}Be), Geomorphol. 195 (2013) 45–52.
[30] M.G.N.M. Neto, As bacias sedimentares de Benguela e Moçamedes, Imprensa Nacional de Angola Boletim 3 (1961) 65–77.
[31] K. Nishiizumi, Preparation of ^{26}Al AMS standards, Nucl. Inst. Meth. Phys. Res. B 223–224 (2004) 388–392.
[32] K. Nishiizumi, M. Imamura, M.W. Caffe, J.R. Southon, R.C. Finkel, J. McAninch, Absolute calibration of ^{10}Be AMS standards, Nucl. Inst. Meth. Phys. Res. B 58 (2007) 403–413.
[33] T.L. Norris, A.J. Gancarz, D.J. Rokop, K.W. Thomas, Half-life of ^{26}Al. Proc. 14th Lunar Planet. Sci. Conf. J. Geophys. Res. 88 (1) (1983) B331–333.
[34] S. Pappu, Y. Gunell, K. Akhilesh, R. Braucher, M. Taieb, F. Demory, N. Thouveny, Early Pleistocene presence of Acheulian hominins in South India, Science 331 (2011) 1596–1599.
[35] T.C. Partridge, D.E. Granger, M.W. Caffee, R.J. Clarke, Lower Pliocene hominid remains from Sterkfontein, Science 300 (2003) 607–612.
[36] D. Quesne, A. Buta-Neto, D. Benard, M. Guiraud, Distribution of Albian clastic deposits in the Benguela basin (Angola): evidence of a Benguela palaeocurrent? Bulletin de la Société Géologique de France 180 (2) (2009) 117–129.
[37] J.A. Sessa, P.M. Callapez, P.A. Dinis, A.J.W. Hendy, Paleoenvironmental and paleobiogeographical implications of a middle Pleistocene mollusc assemblage from the marine terraces of Baía Das Pipas, southwest Angola, J. Paleontol. 87 (6) (2013) 1016–1040.
[38] A.J.L.D.A. Soares, A.T. Visser, The Performance of stabilized pebble bases under light urban traffic in Luanda, Republic of Angola, in: Proceedings of the 26th Southern African Transport Conferenec (SATC 2007), 267–276, 2007.
[39] G. Soares De Carvalho, Alguna problemas dos terraces quaternarias de litoral de Angola, Bol. Ser. Geol. Min. Angola 2 (1961) 5–15.
[40] J.O. Stone, Air pressure and cosmogenic isotope production, J. Geophys. Res. 105 (B10) (2000) 23753–23759.
[41] P. Vermeesch, CosmoCalc: an Excel add-in for cosmogenic nuclide calculations, Geochem. Geophys. Geosyst. 8 (2007) Q08003, https://doi.org/10.1029/2006GC001530.
[42] P. Vermeesch, On the visualisation of detrital age distributions, Chem. Geol. 312–313 (2012) 190–194.
[43] R.T. Walker, M. Telfer, R.L. Kahle, M.W. Dee, B. Kahle, J.-L. Schwenninger, R.A. Sloan, A.B. Watts, Rapid mantle-driven uplift along the Angolan margin in the late Quaternary, Nat. Geosci. 9 (2016) 909–914.
[44] G.K. Ward, S.R. Wilson, Procedures for comparing and combining radiocarbon age determinations: a critique, Archaeometry 20 (1) (1978) 19–31.
[45] W. Zhang, Z. Liu, J. Zheng, S. Zhang, Y. Yu, Experimental study on water sensibility of the Red Sand Foundation in Angola, Engineering Geology for Society and Territory 6 (2015) 229–235.
[46] O. Dauteuil, F. Deschamps, O. Bourgeois, A. Mocquet, F. Guillocheau, Post-breakup evolution and palaeotopography of the North Namibian Margin during the Meso-Cenozoic, Tectonophysics 589 (2013) 103–115.